Physical bounds and summation rules in antenna theory

***Mats Gustafsson* and Christian Sohl**
Dept. of Electrical and Information Technology, Lund University, P.O. Box 118, S-221 00 Lund, Sweden.
{Mats.Gustafsson,Christian.Sohl}@eit.lth.se; fax +46-46 12 99 48.

Abstract

Although the concept of physical bounds for electrically small antennas was first introduced more than half a century ago by Wheeler and Chu it continuous to receive attention and still there is only a partial knowledge of these bounds. Most of the research effort in this field are based on the ideas of a stored energy in the different partial waves as introduced by Chu and, hence, suffers from the same shortcomings. The objective of this paper is to present three alternative approaches to derive physical bounds on antennas that are solely based on the assumptions of linearity, time-translational invariance, causality, and reciprocity. These assumptions are utilized in three different scattering settings to construct various Herglotz functions from which summation rules and associated physical bounds are derived.

1 Introduction

Herglotz (or positive real) functions can be considered as the mathematical background to summation rules. Theses functions are defined as holomorphic mappings from one complex half plane into itself. Cauchy integrals applied to Herglotz functions under the assumption of special asymptotic expansions of the low and high frequency offer summation rules for several electromagnetic problems. In [1–3], a summation rule that relate the extinction cross sections to the polarizability of electromagnetic scatterers is analyzed and *e.g.*, used to derive physical bounds for antennas.

Here, a general lossless single port antenna including a matching network and transmission line is considered [2–4]. The physical bounds and summation rules are solely based on the assumptions of a linear, time-translational invariant, causal, and reciprocal antenna. These assumptions are used to derive various Herglotz functions and corresponding physical bounds in the forward, partial-wave, and transmission line scattering settings as depicted in Fig. 1.

2 Physical bounds on forward scattering

Physical bounds derived from the forward scattering of antennas and general scatterers are thoroughly analyzed in [1–3]. Here, the main results are reviewed together with an outline of the derivation to highlight the similarities with the other bounds presented in this paper. It can be shown that the forward scattering defines a Herglotz function, h, via the optical theorem such that $\sigma_{\rm ext}(k;\hat{\boldsymbol{k}},\hat{\boldsymbol{e}}) = \operatorname{Im} h(k;\hat{\boldsymbol{k}},\hat{\boldsymbol{e}})$ denotes the extinction cross section assiciated with the plane wave $\hat{\boldsymbol{e}}\exp(\mathrm{i}k\hat{\boldsymbol{k}}\cdot\boldsymbol{r})$ [1]. The low- and high-frequency asymptotics of h are $h(k,\hat{\boldsymbol{k}},\hat{\boldsymbol{e}}) = \mathcal{O}(k)$ as $k\to 0$ and $h(k,\hat{\boldsymbol{k}},\hat{\boldsymbol{e}}) = \mathcal{O}(1)$ as $k\to\infty$, respectively. The non-zero k^2-term in the expansion at the origin limits the possible summation rules to

$$\int_0^\infty \frac{\sigma_{\rm ext}(k;\hat{\boldsymbol{k}},\hat{\boldsymbol{e}})}{k^2}\,\mathrm{d}k = \frac{\pi}{2}(\hat{\boldsymbol{e}}^*\cdot\boldsymbol{\gamma}_{\rm e}\cdot\hat{\boldsymbol{e}} + \hat{\boldsymbol{k}}\times\hat{\boldsymbol{e}}^*\cdot\boldsymbol{\gamma}_{\rm m}\cdot\hat{\boldsymbol{k}}\times\hat{\boldsymbol{e}}), \tag{1}$$

where $\boldsymbol{\gamma}_{\rm e}$ and $\boldsymbol{\gamma}_{\rm m}$ denote the electric and magnetic polarizability dyadics, respectively. A corresponding identity more applicable to antenna theory is obtained by introducing the absorption cross section, $\sigma_{\rm a} = \sigma_{\rm a}(k;\hat{\boldsymbol{k}},\hat{\boldsymbol{e}})$, the generalized absorption efficiency,

$$\eta(\hat{\boldsymbol{k}},\hat{\boldsymbol{e}}) = \int_0^\infty \frac{\sigma_{\rm a}(k;\hat{\boldsymbol{k}},\hat{\boldsymbol{e}})}{k^2}\,\mathrm{d}k \Bigg/ \int_0^\infty \frac{\sigma_{\rm ext}(k;\hat{\boldsymbol{k}},\hat{\boldsymbol{e}})}{k^2}\,\mathrm{d}k\ , \tag{2}$$

and the partial directivity, $D = D(k;\hat{\boldsymbol{k}},\hat{\boldsymbol{e}})$, via $\sigma_{\rm a}(k;\hat{\boldsymbol{k}},\hat{\boldsymbol{e}}) = \pi(1-|\varGamma(k)|^2)D(k;-\hat{\boldsymbol{k}},\hat{\boldsymbol{e}}^*)/k^2$. The result is

$$\int_0^\infty \frac{(1-|\varGamma(k)|^2)D(k;\hat{\boldsymbol{k}},\hat{\boldsymbol{e}})}{k^4}\,\mathrm{d}k = \frac{\eta(-\hat{\boldsymbol{k}},\hat{\boldsymbol{e}}^*)}{2}(\hat{\boldsymbol{e}}^*\cdot\boldsymbol{\gamma}_{\rm e}\cdot\hat{\boldsymbol{e}} + \hat{\boldsymbol{k}}\times\hat{\boldsymbol{e}}^*\cdot\boldsymbol{\gamma}_{\rm m}\cdot\hat{\boldsymbol{k}}\times\hat{\boldsymbol{e}}), \tag{3}$$

where an asterisk denotes the complex conjugate.

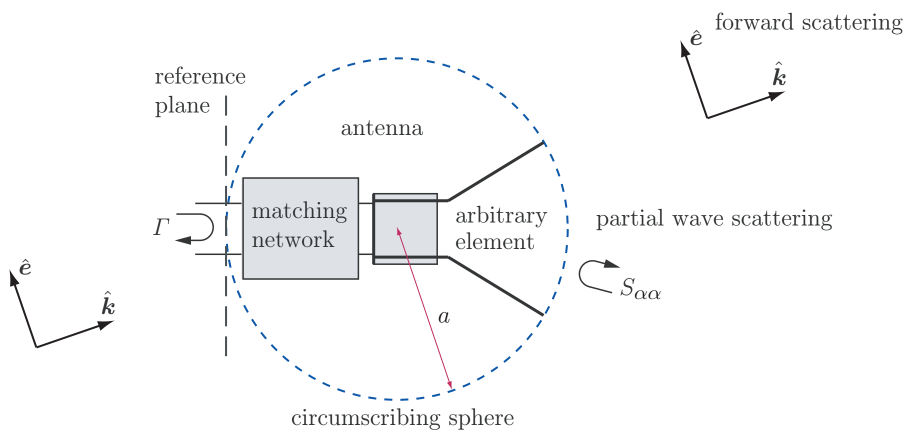

Figure 1: The antenna scattering setup illustrating forward, partial wave, and transmission line scattering.

This identity can be estimated in several different ways [2, 3], *e.g.*, a single resonance model yields

$$\frac{D(k_0;\hat{\boldsymbol{k}},\hat{\boldsymbol{e}})}{Q_{\mathrm{p}}} \leq \frac{\eta(-\hat{\boldsymbol{k}},\hat{\boldsymbol{e}}^*)k_0^3}{2\pi}(\hat{\boldsymbol{e}}^*\cdot\boldsymbol{\gamma}_{\mathrm{e}}\cdot\hat{\boldsymbol{e}}+\hat{\boldsymbol{k}}\times\hat{\boldsymbol{e}}^*\cdot\boldsymbol{\gamma}_{\mathrm{m}}\cdot\hat{\boldsymbol{k}}\times\hat{\boldsymbol{e}}), \tag{4}$$

where Q_{p} denotes the Q-factor of the partial realized gain at the resonance frequency, $k = k_0$.

3 Physical bounds based on partial waves

Consider an antenna system with N local ports and expand the electromagnetic field outside the antenna in incoming and outgoing spherical vector waves (partial waves or modes) [5, 6]. Denote the scattering from an incoming wave to an outgoing wave by $S_{\alpha,\alpha'}(k)$, where $\alpha = \{\tau, s, m, l\}$ for $l = 1, 2, \ldots$, $s = 1, 2$, $m = 0, 1, \ldots, l$, and $\tau = 1, 2$ is the multi-index numbering the different partial waves. The low-frequency expansion of the diagonal elements are $S_{\alpha,\alpha}(k) = 1 + 2\mathrm{i}k^3a^3b_{\alpha,\alpha} + \mathcal{O}(k^4)$ as $k \to 0$, where

$$b_{\alpha,\alpha} = \frac{1}{16\pi^2a^3}\iint \boldsymbol{A}_\alpha(\hat{\boldsymbol{r}})\cdot\boldsymbol{\gamma}_{\mathrm{e}}\cdot\boldsymbol{A}_\alpha(\hat{\boldsymbol{k}})+\hat{\boldsymbol{r}}\times\boldsymbol{A}_\alpha(\hat{\boldsymbol{r}})\cdot\boldsymbol{\gamma}_{\mathrm{m}}\cdot\hat{\boldsymbol{k}}\times\boldsymbol{A}_\alpha(\hat{\boldsymbol{k}})\,\mathrm{d}\Omega\,\mathrm{d}\Omega. \tag{5}$$

Here, $\boldsymbol{A}_\alpha$ denotes the spherical vector harmonics [5, 6], $\cos(m\phi)$ and $\sin(m\phi)$ are used as azimuthal basis functions, and the modes labeled by $\tau = 1$ and $\tau = 2$ identify TE modes (magnetic 2^l-poles) and TM modes (electric 2^l-poles), respectively. The scattering coefficients are bounded in magnitude by unity and are holomorphic for $\operatorname{Im} k > 0$, so $\mathrm{i}\ln S_{\alpha,\alpha}(k)$ can be used to define a Herglotz function. However, as $S_{\alpha,\alpha}(k)$ in general has zeros, k_n, in the upper half of the complex k-plane it is necessary to remove these by extracting the associated Blaschke product [7].

Integration over a large semi-circle in the upper half plane yields the following summation rules:

$$\int_0^\infty \frac{1}{k^2}\ln\frac{1}{|S_{\alpha,\alpha}(k)|}\,\mathrm{d}k \leq \pi a + \pi\sum_n \operatorname{Im}\frac{1}{k_n},\qquad \int_0^\infty \frac{1}{k^4}\ln\frac{1}{|S_{\alpha,\alpha}(k)|}\,\mathrm{d}k = \pi a^3 b_{\alpha,\alpha} + \frac{\pi}{3}\sum_n \operatorname{Im}\frac{1}{k_n^3}. \tag{6}$$

The first summation rule in (6) depends on the smallest circumscribing sphere of radius a, see Fig. 1. The second identity in (6) includes the shape and material properties of the antenna as quantified by the polarizability dyadics in (5). These integral identities can be used to derive various bounds on the scattering coefficients and bandwidth, *cf.*, the Fano theory [8, 9]. The narrow bandwidth approximation, $B \ll 1$, bound of (6) is

$$\frac{B\ln S_0^{-1}}{\pi} \leq k_0a - \sqrt[3]{q+p} + \sqrt[3]{q-p} = \frac{(1+3b_{\alpha,\alpha})}{3}k_0^3a^3 + \mathcal{O}(k_0^5a^5)\quad \text{as } k_0a \to 0, \tag{7}$$

where $p = 3k_0a(1-b_{\alpha,\alpha}k_0^2a^2)/2$, $q = \sqrt{1+p^2}$, $S_0 = \max_{k_1\leq k\leq k_2}|S_{\alpha,\alpha}|$, $k_0 = (k_1+k_2)/2$, and $B = (k_2-k_1)/k_0$.

4 Summation rules for the antenna input impedance

The input impedance, $Z = R_0(1+\Gamma)/(1-\Gamma)$, is defined in the reference plane of a transmission line with characteristic impedance R_0, see Fig. 1, and generates a Herglotz function. Assume that $Z = R + \mathrm{j}X$ is well defined for all finite frequencies and can be expanded in asymptotic series at $\omega = 0$ and $\omega = \infty$, where ω denotes the angular frequency and $\mathrm{j} = -\mathrm{i}$. Specifically, the low frequency expansion is assumed to have the form $Z(\omega) = 1/(\mathrm{j}\omega C) + \mathrm{j}\omega L + \mathcal{O}(\omega^2)$ as $\omega \to 0$, with $C, L > 0$ and the high-frequency asymptotic is assumed to be $Z(\omega) = \mathrm{j}\omega L_\infty + \mathcal{O}(1)$ as $\omega \to \infty$, where $L_\infty \leq L$. The corresponding admittance, $Y = 1/Z = G + \mathrm{j}B$, has the expansions $Y(\omega) = \mathrm{j}\omega C + \mathrm{j}\omega^3 LC^2 + \mathcal{O}(\omega^4)$ as $\omega \to 0$, and $Y(\omega) = \omega B_\infty + \mathcal{O}(1)$ as $\omega \to \infty$. Integrate $Z(\omega)/\omega^2$, $Y(\omega)/\omega^2$, and $Y(\omega)/\omega^4$ over a large semi-circle to get the following summation rules:

$$\int_0^\infty \frac{R(\omega)}{\omega^2}\,\mathrm{d}\omega = \frac{\pi}{2}(L - L_\infty), \quad \int_0^\infty \frac{G(\omega)}{\omega^2}\,\mathrm{d}\omega = \frac{\pi}{2}(C - B_\infty), \quad \int_0^\infty \frac{G(\omega)}{\omega^4}\,\mathrm{d}\omega = \frac{\pi}{2}LC^2. \tag{8}$$

It is often easier to interpret the corresponding identities for the reflection coefficient, Γ, viz

$$\int_0^\infty \frac{\ln|\Gamma(\omega)|^{-1}}{\omega^2}\,\mathrm{d}\omega = \pi C R_0 + \pi \sum_n \operatorname{Im}\frac{1}{\omega_n}, \quad \int_0^\infty \frac{\ln|\Gamma(\omega)|^{-1}}{\omega^4}\,\mathrm{d}\omega = \pi C R_0 \left(CL - \frac{C^2R_0^2}{3}\right) + \frac{\pi}{3}\sum_n \operatorname{Im}\frac{1}{\omega_n^3}, \tag{9}$$

where ω_n denotes the complex-valued zeros of Γ. The narrow-bandwidth approximation reads

$$\frac{B\ln\Gamma_0^{-1}}{\pi} \leq CR_0\omega_0 - \sqrt[3]{q+p} + \sqrt[3]{q-p} = C^2 L R_0 \omega_0^3 + \mathcal{O}(\omega_0^5), \quad \text{as } \omega_0 \to 0 \tag{10}$$

where $\Gamma_0 = \max_{\omega_1 \leq \omega \leq \omega_2} |\Gamma|$, $\omega_0 = (\omega_1 + \omega_2)/2$, $B = (\omega_2 - \omega_1)/\omega_0$, $p = 3CR_0\omega_0(1 - (CL - C^2R_0^2/3)\omega_0^2)/2$ and $q = \sqrt{1+p^2}$. The corresponding magnetic antenna with $1/C = 0$ is analyzed with an analogous low frequency expansion for the admittance, $Y = 1/Z$.

5 Numerical examples

Cylindrical dipole antennas with semi-axis ratios $\ell/d = 1000, 500, 100$ and capacitively loaded dipoles with a length to top diameter ratio $\ell/d = 10, 1$ are utilized to illustrate the bounds, see Tab. 1. The antennas are center fed with a simple gap model in the MoM simulations to determine the impedances and radiation patterns from which the capacitance, inductance, resonance frequency, radiation resistance, and Q-factor are estimated. The corresponding polarizability dyadics are also calculated with the MoM. In Tab. 1, the reciprocals of (7) and (10) are used to simplify the comparison with the Q-factors [9], and the Chu bound $Q_{\text{Chu}} = (k_0a)^{-3} + (k_0a)^{-1}$ is included [10].

6 Conclusions

The physical bounds introduced in this paper, generalized in many aspects the classical bounds by Chu. The new bounds are based on restrictions on the static or low-frequency properties of the antennas giving the interpretation of high-pass filters. It also makes the identities most interesting for electrically small antennas although they are valid for a much larger class of structures. The different approaches considered have their strength and weaknesses but they all give insight into the physics of small antennas. It is seen that the forward scattering approach (3) is very accurate for the antennas in Tab. 1. However, it is important to remember that the results in Tab. 1 are based on a priori knowledge of the generalized absorption efficiency η, and even though $\eta \approx 0.5$ for many antennas in general it can take any value between 0 and 1. Moreover, the polarization dependence in the forward scattering approach offers additional information about the effect of polarization diversity with possible applications to MIMO antennas.

The diversity in MIMO antennas are better treated by the partial waves in (6). However, these bounds are not as tight as the forward scattering bounds for the antennas in Tab. 1. The main deficiency originates from the compensation of the non-causality as is quantified by the radius of the smallest circumscribing sphere (6) making these comparable to the Chu bounds [10]. It is also realized that the approaches in (3) and (6) are less suited for cases where the antennas are placed in the vicinity of a large object where they only constitute a fraction of volume as this in general cause both a small absorption efficiency and a large circumscribing sphere. The third approach based in the input impedance is

Antenna					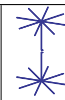
ℓ/d	1000	500	100	10	1
γ_{zz}/a^3	0.71	0.81	1.2	2.3	5.1
$C/(\epsilon_0 a)$	0.54	0.62	0.92	1.4	3.1
$L/(\mu_0 a)$	0.64	0.56	0.37	0.40	0.72
$k_0 a = \omega_0 a/\mathrm{c}_0$	1.51	1.51	1.48	1.17	0.63
R_0/η_0	0.19	0.19	0.19	0.17	0.04
$\max D$	1.64	1.64	1.64	1.61	1.50
η	0.51	0.51	0.51	0.51	0.50
$Q_0 = \omega_0 \lvert Z' \rvert / 2R_0$	8.2	7.4	5.3	5.1	14
Q_{p}	8.2	7.4	5.2	5.1	14
$\pi/B/\ln S_0^{-1}$	2.1	2.0	2.0	2.7	8.8
$\pi/B/\ln \varGamma_0^{-1}$	8.3	7.2	5.3	4.8	14
Q_{Chu}	1	1	1	1.5	5.5

Table 1: Numerical results of various antennas where η_0 and c_0 denote the wave impedance and phase velocity of free space, respecively.

better for this case as it is formulated in the intrinsic antenna parameters. Its main deficiency, however, is that it is difficult to relate the limiting coefficients, *e.g.*, C and L, to the available antenna geometry.

References

[1] C. Sohl, M. Gustafsson, and G. Kristensson. "Physical limitations on broadband scattering by heterogeneous obstacles". *J. Phys. A: Math. Theor.*, vol. 40, pp. 11165–11182, 2007.

[2] M. Gustafsson, C. Sohl, and G. Kristensson. "Physical limitations on antennas of arbitrary shape". *Proc. R. Soc. A*, vol. 463, pp. 2589–2607, 2007.

[3] C. Sohl and M. Gustafsson. "A priori estimates on the partial realized gain of UWB-antennas". Tech. Rep. LUTEDX/(TEAT-7160)/1–19/(2007), Lund University, Department of Electrical and Information Technology, P.O. Box 118, S-221 00 Lund, Sweden, 2007. Http://www.eit.lth.se.

[4] A. D. Yaghjian and S. R. Best. "Impedance, bandwidth, and Q of antennas". *IEEE Trans. Antennas Propagat.*, vol. 53(4), pp. 1298–1324, 2005.

[5] J. E. Hansen, ed. *Spherical Near-Field Antenna Measurements*. No. 26 in IEE electromagnetic waves series. Stevenage, UK: Peter Peregrinus Ltd., 1988. ISBN: 0-86341-110-X.

[6] M. Gustafsson and S. Nordebo. "Characterization of MIMO antennas using spherical vector waves". *IEEE Trans. Antennas Propagat.*, vol. 54(9), pp. 2679–2682, 2006.

[7] H. M. Nussenzveig. *Causality and dispersion relations*. London: Academic Press, 1972.

[8] R. M. Fano. "Theoretical limitations on the broadband matching of arbitrary impedances". *Journal of the Franklin Institute*, vol. 249(1,2), pp. 57–83 and 139–154, 1950.

[9] M. Gustafsson and S. Nordebo. "Bandwidth, Q-factor, and resonance models of antennas". *Progress in Electromagnetics Research*, vol. 62, pp. 1–20, 2006.

[10] L. J. Chu. "Physical limitations of omni-directional antennas". *Appl. Phys.*, vol. 19, pp. 1163–1175, 1948.